IEEE Access
Multidisciplinary | Rapid Review | Open Access Journal

Received May 18, 2018, accepted June 19, 2018, date of publication June 27, 2018, date of current version August 15, 2018.

Digital Object Identifier 10.1109/ACCESS.2018.2851076

Spectral-Efficient Generalized Spatial Modulation Based Hybrid Dimming Scheme With LACO-OFDM in VLC

TENGJIAO WANG[1], FANG YANG[1,2], (Senior Member, IEEE), LING CHENG[3], (Senior Member, IEEE), AND JIAN SONG[1,2], (Fellow, IEEE)

[1]Department of Electronic Engineering, Beijing National Research Center for Information Science and Technology, Tsinghua University, Beijing 100084, China
[2]Key Laboratory of Digital TV System of Guangdong Province and Shenzhen City, Research Institute of Tsinghua University in Shenzhen, Shenzhen 518057, China
[3]School of Electrical and Information Engineering, University of the Witwatersrand, Johannesburg 2000, South Africa

Corresponding author: Fang Yang (e-mail: fangyang@tsinghua.edu.cn)

This work was supported in part by the International Science and Technology Cooperation Program—National Key Research and Development Program of China under Grant 2017YFE0113300 and in part by the South African National Research Foundation under Grant 114626.

ABSTRACT Visible light communication (VLC) is regarded as one of the promising candidates to complement the conventional radio frequency communication as it can potentially perform communication and illumination simultaneously. Recently, VLC is combined with the generalized spatial modulation (GenSM) technology to improve spectral and energy efficiencies. In order to provide high-speed communication and flexible dimming control simultaneously, in this paper, a spectral-efficient GenSM-based hybrid dimming scheme with layered asymmetrically clipped optical OFDM is proposed for VLC, which combines the spatial-domain and time-domain dimming strategies. The channel capacities of the proposed scheme are analyzed and the closed-form expressions of the channel capacity are derived in both the rich scattering scenario and highly correlated scenario. According to the required illumination level, the spatial-domain and time-domain strategies are realized based on the maximization of the channel capacity. Simulation results substantiate the superior performance of the proposed dimming scheme over the state-of-art dimming schemes.

INDEX TERMS Channel capacity optimization, generalized spatial modulation, hybrid dimming control, multiple-input multiple-output, visible light communication.

I. INTRODUCTION

Visible light communication (VLC) is an emerging wireless communication technology which utilizes the ubiquitous light-emitting diodes (LEDs) network to provide promising communication services [1], [2]. Compared to traditional radio frequency (RF) communications, VLC takes advantage of the wide unlicensed visible light spectrum to facilitate high-capacity communications with less inter-cell interference [3], [4], and thus has attracted considerable academic and industrial attentions [5].

Recently, VLC is combined with multiple-input multiple-output (MIMO) technology with spatial modulation (SM) to improve spectral and energy efficiencies [6]. As an extension of MIMO, SM based VLC only activates one LED in the LED arrays in a time slot to improve energy efficiency [7]. The generalized spatial modulation (GenSM) is a generalization of SM, which activates more than one LEDs at the same time to further improve the spectral efficiency [8]. So far, the combination of GenSM and VLC has been investigated in many aspects, including symbol design [9], receiver design [10], dual-mode communications [11], physical layer security [12] and so on.

Other than communication, illumination is the other basic function of VLC [13]. However, illumination has an adverse effect on communication. Since intensity modulation (IM) and direct detection (DD) are widely used in VLC, the intensity should be carefully controlled within the dynamic range of the LEDs [14]. Different illumination requirements will reduce the usable intensity range and thus influence the quality of communication. As a result, different kinds of dimming techniques are formulated to obtain a better balance between illumination and communication, such as modulation based

2169-3536 © 2018 IEEE. Translations and content mining are permitted for academic research only.
Personal use is also permitted, but republication/redistribution requires IEEE permission.
See http://www.ieee.org/publications_standards/publications/rights/index.html for more information.

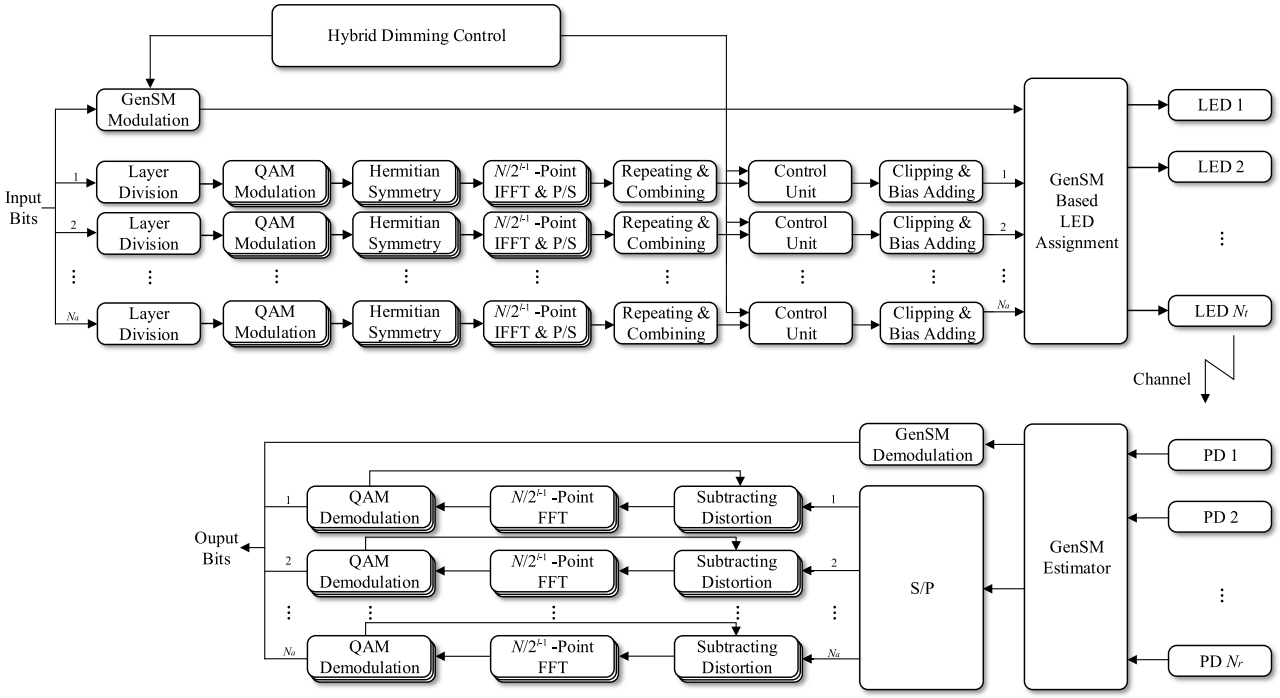


FIGURE 1. The system model of the GenSM based hybrid dimming scheme.

dimming techniques [15], coding based dimming techniques [16] and adaptive dimming techniques [17]. Recently, a spatial dimming technology is proposed in [18], which utilizes the number of glared LEDs in an LED lamp to represent different illumination level for the direct current biased optical OFDM (DCO-OFDM) system. Since the bias level is not adjusted to the required illumination level, the clipping noise of the spatial dimming method is mitigated. Based on this, a hybrid dimming control scheme with spatial dimming is further proposed in [19].

In this paper, a spectral-efficient GenSM based hybrid dimming scheme with layered asymmetrically clipped optical OFDM (LACO-OFDM) is proposed for VLC, where the spatial-domain dimming strategy and the time-domain dimming strategy are combined to achieve the desired illumination level. The channel capacities of the proposed scheme are analyzed and closed-form expressions of the channel capacity are further derived in both the rich scattering scenario and the highly correlated scenario. Based on the maximization of the proposed expressions, the optimal number of activated LEDs is determined to realize spatial-domain dimming. Then the time-domain dimming strategy is applied to further adjust the illumination according to the requirements. In the end, the superior performance of the proposed hybrid dimming scheme is verified through numerical simulations.

The rest of the paper is organized as follows. In Section II, the system model of the GenSM based hybrid dimming scheme with LACO-OFDM is investigated. In Section III, the channel capacity of the system is analyzed and the optimal number of activated antennas is derived based on the maximization of the channel capacity in both the rich scattering scenario and the highly correlated scenario. Then the novel spectral efficient hybrid dimming scheme is proposed in Section IV based on the optimization results in the two scenarios. Numerical simulation results are provided in Section V and conclusions are drawn in Section VI.

Notation: Column vectors and matrices are denoted by lowercase and uppercase boldface letters; Conjugate transposition and transposition are denoted by $(\cdot)^{\mathrm{H}}$ and $(\cdot)^{\mathrm{T}}$, respectively; $\binom{\cdot}{\cdot}$ denotes the binomial coefficient.

II. SYSTEM MODEL

In this section, the system model of the GenSM based multi-LED VLC, the positive and negative LACO-OFDMs, and the channel gain of VLC will be investigated in detail.

A. GENSM BASED MULTI-LED VLC

We consider a GenSM based VLC communication system where the transmitter is equipped with N_t LEDs and the receiver is equipped with N_r photo detectors (PDs) as shown in Fig. 1. OFDM is adopted in the system since it has shown great favor for VLC [20].

In the VLC transmitter, the input bits are divided into two parts. In the first part, the information bits are used to choose the activated LEDs according to the GenSM modulation. Suppose N_a LEDs are activated at the same time to transmit signals, $\log_2\binom{N_t}{N_a}$ bits of information can be transmitted through the indices of the LEDs according to the principle of GenSM [8]. The GenSM modulation results are used to assign the corresponding LEDs in the LED arrays.

The other part of information bits are divided into N_a streams and each stream is modulated according to the principle of LACO-OFDM, which will be explained in detail in the next subsection. Since IM/DD is widely adopted in VLC communication system, a Hermitian symmetry block is necessary before the inverse fast Fourier transform (IFFT) block to ensure that the time-domain symbol after IFFT is real. Then the time-domain symbols are clipped and added by the direct current bias to ensure that the transmitted symbols are positive and within the dynamic range of the LEDs. The n-th transmitted symbol in the i-th stream is denoted as $x_{i,n}$. Thus the transmission function of the GenSM based hybrid dimming system is given as

$$\mathbf{y}_n = \mathbf{H}_n \mathbf{x}_n + \mathbf{w}_n, \tag{1}$$

where $\mathbf{y}_n \in \mathbb{R}^{N_r \times 1}$ is the n-th received signal at the VLC receiver. $\mathbf{H}_n \in \mathbb{R}^{N_r \times N_t}$ is the VLC channel matrix when transmitting the n-th symbol. $\mathbf{w}_n \in \mathbb{R}^{N_r \times 1} \sim \mathcal{N}(\mathbf{0}, \sigma_{\mathrm{n}}^2 \mathbf{I}_{N_r})$ represents the additive white Gaussian noise (AWGN) with variance σ_{n}^2 for the n-th symbol. $\mathbf{x}_n \in \mathbb{R}^{N_t \times 1}$ is the n-th transmitted VLC symbol. Since GenSM is adopted, only N_a elements in $\mathbf{x}_n$ are non-zero, which can be expressed as

$$\mathbf{x}_n = [0, \ldots, x_{1,n}, \ldots, x_{N_a,n}, \ldots, 0]^{\mathrm{T}}, \tag{2}$$

where the indexes of $x_{i,n}$, $i \in [1, N_a]$ are based on the chosen activated antennas.

B. POSITIVE AND NEGATIVE LACO-OFDMS

In literature, many kinds of OFDM schemes have been proposed for VLC, such as DCO-OFDM [21], ACO-OFDM [22], hybrid ACO-OFDM [23], LACO-OFDM [24] and so on. The spectral efficient LACO-OFDM method is adopted in this paper to demonstrate the superior performance of the proposed hybrid dimming scheme.

LACO-OFDM combines several layers of ACO-OFDM signals to achieve better spectral efficiency, where N subcarriers and L layers are considered in this paper. In the l-th layer, the quadrature amplitude modulation (QAM) symbols are only transmitted on the $2^{l-1}(2k+1)$-th ($k = 0, 1, \ldots, N/2^l - 1$) subcarriers to satisfy the Hermitian symmetry [25]. Thus in the i-th stream and the l-th layer, only $N/2^{l+1}$ independent frequency-domain symbols are modulated on the subcarriers. It is proven in [24] that the time-domain symbol in the l-th layer can be derived by the repetition of the $N/2^{l-1}$ IFFT result of $\mathbf{S}_i^{(l)}$, which is given as

$$\mathbf{S}_i^{(l)} = [0, S_{i,1}^{(l)}, 0, S_{i,3}^{(l)}, \ldots, S_{i,N/2^l-1}^{(l)}, 0, S_{i,N/2^l-1}^{(l)*}, \ldots, 0, S_{i,1}^{(l)*}], \tag{3}$$

where $S_{i,k}^{(l)}$ denotes the k-th frequency-domain symbol in the i-th stream and l-th layer. Then the $N/2^{l-1}$-point IFFT is applied to each layer to derive the time-domain symbols, which is

$$s_{i,n}^{(l)} = \frac{1}{\sqrt{N/2^{l-1}}} \sum_{k=1}^{N/2^{l-1}} S_{i,k}^{(l)} e^{\frac{j2\pi nk}{N/2^{l-1}}}, \tag{4}$$

where $s_{i,n}^{(l)}$ denotes the n-th time-domain symbol in the i-th stream and l-th layer. After IFFT, the time-domain symbols satisfy the anti-symmetry property, which is

$$s_{i,n}^{(l)} = -s_{i,n+N/2^l}^{(l)}, \quad (0 < n < \frac{N}{2^l}). \tag{5}$$

Then the time-domain symbols in the l-th layer are repeated by 2^{l-1} times to get the same length N. The LACO-OFDM symbols are derived by combining the L-layer symbols in the same stream, which can be expressed as

$$s_{i,n}^{\mathrm{LACO}} = \sum_{l=1}^{L} \gamma(s_{i,n}^{(l)}, 2^{l-1}), \tag{6}$$

where $\gamma(a, b)$ denotes the repeating operator which means repeating a by b times. Because of the anti-symmetry property in (5), either the positive part or the negative part of the time-domain symbols can be clipped without any information loss to derive unipolar symbols [26]. The positive and negative clipped LACO-OFDM symbols are denoted as $s_{i,n}^{\mathrm{PLACO}}$ and $s_{i,n}^{\mathrm{NLACO}}$, which are given as

$$s_{i,n}^{\mathrm{PLACO}} = \begin{cases} s_{i,n}^{\mathrm{LACO}}, & s_{i,n}^{\mathrm{LACO}} \geq 0 \\ 0, & s_{i,n}^{\mathrm{LACO}} < 0, \end{cases} \tag{7}$$

and

$$s_{i,n}^{\mathrm{NLACO}} = \begin{cases} 0, & s_{i,n}^{\mathrm{LACO}} > 0 \\ s_{i,n}^{\mathrm{LACO}}, & s_{i,n}^{\mathrm{LACO}} \leq 0. \end{cases} \tag{8}$$

In the bias addition block, the positive and negative LACO-OFDM symbols are rescaled and added to the minimum and maximum currents of the LEDs dynamic range, respectively. Thus the n-th transmitted symbol in the i-th stream is given as

$$x_{i,n}^{\mathrm{PLACO}} = \begin{cases} I_{\mathrm{H}}, & s_{i,n}^{\mathrm{LACO}} > \dfrac{I_{\mathrm{H}} - I_{\mathrm{L}}}{\beta_i} \\ \beta_i s_{i,n}^{\mathrm{LACO}} + I_{\mathrm{L}}, & 0 \leq s_{i,n}^{\mathrm{LACO}} \leq \dfrac{I_{\mathrm{H}} - I_{\mathrm{L}}}{\beta_i} \\ I_{\mathrm{L}}, & s_{i,n}^{\mathrm{LACO}} < 0, \end{cases} \tag{9}$$

and

$$x_{i,n}^{\mathrm{NLACO}} = \begin{cases} I_{\mathrm{H}}, & s_{i,n}^{\mathrm{LACO}} > 0 \\ \beta_i s_{i,n}^{\mathrm{LACO}} + I_{\mathrm{H}}, & \dfrac{I_{\mathrm{L}} - I_{\mathrm{H}}}{\beta_i} \leq s_{i,n}^{\mathrm{LACO}} \leq 0 \\ I_{\mathrm{L}}, & s_{i,n}^{\mathrm{LACO}} \leq \dfrac{I_{\mathrm{L}} - I_{\mathrm{H}}}{\beta_i}, \end{cases} \tag{10}$$

where I_{L} and I_{H} denote the allowed minimum and maximum currents in the dynamic range of the LEDs. β_i denotes the scaling factor in the i-th stream.

Since the average amplitude of the two kinds of symbols are different, the proportion of the two symbols in a frame can be utilized to control the illumination of the system, which will be explained in detail in Section IV.

C. CHANNEL GAIN OF VLC

In the VLC communication system, the channel gain can be divided into the line-of-sight (LOS) part and the non-LOS part [19]. According to the propagation characteristic of VLC, the dominant LOS channel gain can be expressed as

$$h_{LOS} = \begin{cases} \frac{(m+1)A}{2\pi d^2} g(\psi)\cos^m(\phi)\cos(\psi), & 0 < \psi < \Psi_c \\ 0, & \psi > \Psi_c, \end{cases} \tag{11}$$

where d and A denote the transmit distance and the area of PDs. ϕ, ψ and Ψ_c denote the angle of irradiance, the angle of incidence and the semiangle of the receiver field of vision (FOV), respectively. The Lambert order and the optical concentrator gain are denoted as m and $g(\phi)$, which are further expressed as

$$m = -\frac{\ln 2}{\ln(\cos \Phi_{1/2})}, \tag{12}$$

and

$$g(\psi) = \begin{cases} \frac{n_r^2}{\sin^2 \Psi_c}, & 0 \le \psi \le \Psi_c \\ 0, & \psi \ge \Psi_c, \end{cases} \tag{13}$$

where $\Phi_{1/2}$ is the semiangle of the transmitter and n_r is the refractive index.

The non-LOS links introduced by the reflection from the walls, floors and other objects, also affect the channel gain of VLC [27], which influence the correlation of the channel gain between different LEDs and PDs. In this paper, the rich scattering scenario where plenty of non-LOS links exist and the LEDs are not so close to each other, and the highly correlated scenario where only the LOS link exists and the LEDs are very close, are investigated respectively.

III. THEORETICAL CHANNEL CAPACITY ANALYSIS

In this section, the channel capacity of the proposed GenSM based VLC system is analyzed, which can be quantified through the mutual information between the transmitted symbols and the received symbols.

In GenSM based system, the mutual information can be decomposed due to the chain rule of mutual information [28],

$$I(\mathbf{x}, x^{\text{index}}; \mathbf{y}) = I(\mathbf{x}; \mathbf{y}|x^{\text{index}}) + I(x^{\text{index}}; \mathbf{y}), \tag{14}$$

where x^{index} denotes the indices of the activated LEDs. It can be seen that the total mutual information is decomposed into two parts. The first part $I(\mathbf{x}; \mathbf{y}|x^{\text{index}})$ represents the mutual information carried by the QAM symbols and the second part $I(x^{\text{index}}; \mathbf{y})$ represents the mutual information carried by the spatial-domain symbols.

The mutual information carried by the spatial-domain symbols is denoted as $I(x^{\text{index}}; \mathbf{y})$, which has no closed-form expression according to [28]. Since high SNR is generally considered in real VLC system, the approximation in the high SNR region is utilized to derive the mutual information of the proposed scheme [29], which is

$$I(x^{\text{index}}; \mathbf{y}) = \log_2 N_c = \log_2 \binom{N_t}{N_a} = \log_2\left(\frac{N_t!}{N_a!(N_t - N_a)!}\right), \tag{15}$$

where N_c denotes the number of different spatial-domain symbols.

In $I(\mathbf{x}; \mathbf{y}|x^{\text{index}})$, since the spatial-domain symbol is given, the mutual information is similar to the MIMO scenario, which is relevant to the channel correlation.

A. RICH SCATTERING SCENARIO

In the rich scattering scenario, the channels of the LEDs and PDs are independent with each other. Suppose the diagonalization precoding is applied to the transmitter, the total mutual information in each layer of LACO-OFDM can be derived by the sum of N_a independent equivalent channels, which is given by

$$I(\mathbf{x}; \mathbf{y}|x^{\text{index}}) = \frac{1}{N_c} \sum_{m=1}^{N_c} \sum_{u \in \Omega_m} \log_2\left(1 + \frac{P_{u,m}\sigma_{u,m}^2}{\sigma_{\text{n}}^2}\right), \tag{16}$$

where $N_c = \binom{N_t}{N_a}$ denotes the total number of spatial-domain symbols. Ω_m denotes the set of indices of the activated LEDs in the m-th spatial-domain symbol. $P_{u,m}$ denotes the power allocated to the u-th LED in Ω_m. $\sigma_{u,m}$ and σ_{n}^2 denote the singular value of the channel matrix $\mathbf{H}$ and the variance of the noise, respectively.

Since LACO-OFDM is adopted in this scheme, due to the Hermitian symmetry requirement, only $N/2^{l+1}$ subcarriers are utilized to transmit independent information in the l-th layer. Thus the total channel capacity is derived as the sum of all the layers, which is given as

$$C_{\text{R}} = \sum_{l=1}^{L} \frac{W}{2^{l+1}} \left(\frac{1}{N_c} \sum_{m=1}^{N_c} \sum_{u \in \Omega_m} \log_2\left(1 + \frac{P_{u,m}\sigma_{u,m}^2}{\sigma_{\text{n}}^2}\right) + \log_2 \frac{N_t!}{N_a!(N_t - N_a)!}\right), \tag{17}$$

which can be further simplified as

$$C_{\text{R}} = \frac{\alpha_L W}{N_c} \sum_{m=1}^{N_c} \sum_{u \in \Omega_m} \log_2\left(1 + \frac{P_{u,m}\sigma_{u,m}^2}{\sigma_{\text{n}}^2}\right) + \alpha_L W \log_2 \frac{N_t!}{N_a!(N_t - N_a)!}, \tag{18}$$

where W denotes the whole bandwidth of the system and α_L denotes the multi-layer gain coefficient, which is given as

$$\alpha_L = \sum_{l=1}^{L} \frac{1}{2^{l+1}} = \frac{2^L - 1}{2^{L+1}}. \tag{19}$$

B. HIGHLY CORRELATED SCENARIO

In the highly correlated scenario, the channels of LEDs and PDs are highly correlated with each other and the rank of the channel matrix degenerates to 1. Thus with the diagonalization precoding, only one $\sigma_{u,m}$ in the m-th spatial-domain symbol is non-zero. As a result, the channel capacity is derived as

$$C_{\mathrm{H}} = \frac{\alpha_L W}{N_c}\sum_{m=1}^{N_c}\log_2(1+\frac{P_{1,m}\sigma_{1,m}^2}{\sigma_{\mathrm{n}}^2}) + \alpha_L W \log_2 \frac{N_t!}{N_a!(N_t-N_a)!}, \quad (20)$$

where $\sigma_{1,m}$ denotes the non-zero singular value of the channel matrix and $P_{1,m}$ denotes the power allocated to the corresponding LED. The multi-layer gain coefficient α_L is the same as that in (19).

IV. PROPOSED HYBRID DIMMING SCHEME

In this section, the proposed GenSM based hybrid dimming scheme is explained in detail, which consists of two steps. In the first step, the optimal power allocation and the optimal number of activated LEDs are derived to realize spatial-domain dimming strategy based on the maximization of the channel capacity. In the second step, the proportion of the symbols using positive and negative LACO-OFDMs is determined to further adjust the illumination level to meet the requirements.

A. GENSM BASED SPATIAL-DOMAIN DIMMING

In the first step, the spatial-domain dimming strategy is implemented based on the channel capacity maximization. Since the channel capacity is relevant to the channel correlation, the strategies in the rich scattering scenario and the highly correlated scenario are discussed respectively.

1) RICH SCATTERING SCENARIO

In the rich scattering scenario, in order to maximize the channel capacity, the power allocation problem should be solved. It can be seen from (18) that the second term of the channel capacity is independent of $P_{u,m}$, thus the power allocation for channel capacity maximization can be formulated as

$$\max_{P_{u,m}} \frac{\alpha_L W}{N_c}\sum_{m=1}^{N_c}\sum_{u\in\Omega_m}\log_2(1+\frac{P_{u,m}\sigma_{u,m}^2}{\sigma_{\mathrm{n}}^2})$$
$$s.t.\ \sum_{u\in\Omega_m} P_{u,m} = P, \quad m=1,2,\ldots,N_c, \quad (21)$$

where P denotes the total transmit power at the transmitter. The Lagrange multiplier method is utilized to derive the optimal power allocation. The Lagrange function can be written as

$$\mathcal{L}(P_{1,m},\ldots,P_{N_a,m},\lambda_1,\ldots,\lambda_{N_c}) = \frac{\alpha_L W}{N_c}\sum_{m=1}^{N_c}\sum_{u\in\Omega_m}\log_2(1+\frac{P_{u,m}\sigma_{u,m}^2}{\sigma_{\mathrm{n}}^2}) + \sum_{m=1}^{N_c}\lambda_m(\sum_{u\in\Omega_m}P_{u,m}-P). \quad (22)$$

By solving the Lagrange problem, since $P_{u,m}$ should be positive, the optimal power allocation can be derived as

$$P_{u,m} = (\mu - \frac{\sigma_{\mathrm{n}}^2}{\sigma_{u,m}^2})^+, \quad (23)$$

$$\mu = \frac{P+\sum_{i=1}^{M_m}\frac{\sigma_{\mathrm{n}}^2}{\sigma_{u,m}^2}}{M_m}, \quad (24)$$

where $(x)^+ = \{x(x>0); 0(x\le 0)\}$ denotes the positive part function. M_m denotes the number of non-zero $P_{u,m}$ in the m-th spatial-domain symbol. These optimal power allocation factors can be derived by the traditional iterative water-filling algorithm. According to the procedure of the algorithm, the optimization of one factor will not decrease the contributions of other factors. Thus the objective function is non-decreasing in each iteration. So the algorithm eventually will reach the optimal solutions. The derived power allocation can be taken back to (18) to obtain the channel capacity.

Then the number of activated LEDs is derived based on the maximization of the channel capacity. The first term of (18) can be simplified on condition that the channel capacity remains the same with different spatial-domain symbols. Thus without loss of generality, the first spatial-domain symbol is utilized to derive the simplification, which is expressed as

$$\frac{\alpha_L W}{N_c}\sum_{m=1}^{N_c}\sum_{u\in\Omega_m}\log_2(1+\frac{P_{u,m}\sigma_{u,m}^2}{\sigma_{\mathrm{n}}^2}) \approx \frac{\alpha_L W}{N_c}\times N_c\sum_{u\in\Omega_1}\log_2(1+\frac{P_{u,1}\sigma_{u,1}^2}{\sigma_{\mathrm{n}}^2}) \approx \alpha_L W\sum_{u=1}^{N_a}\log_2(1+\frac{P_{u,1}\sigma_{u,1}^2}{\sigma_{\mathrm{n}}^2}). \quad (25)$$

The Stirling's approximation can be further applied to approximate the factorial in the second term of (18), which can be expressed as

$$\alpha_L W\log_2\frac{N_t!}{N_a!(N_t-N_a)!} \approx \alpha_L W[(N_t+\frac{1}{2})\log_2(N_t) - (N_t-N_a+\frac{1}{2})\log_2(N_t-N_a) - \frac{\log_2(2\pi)}{2} - (N_a+\frac{1}{2})\log_2(N_a)]. \quad (26)$$

Thus the channel capacity can be approximated as

$$C_{\mathrm{R}} \approx \alpha_L W[\sum_{u=1}^{N_a}\log_2(1+\frac{P_{u,1}\sigma_{u,1}^2}{\sigma_{\mathrm{n}}^2}) + (N_t+\frac{1}{2})\log_2(N_t) - (N_t-N_a+\frac{1}{2})\log_2(N_t-N_a) - (N_a+\frac{1}{2})\log_2(N_a) - \frac{\log_2(2\pi)}{2}]. \quad (27)$$

Then the optimal N_a can be derived based on the maximization of (27) through many numerical iterative methods, such as the steepest descent algorithm and the conjugate gradient method.

2) HIGHLY CORRELATED SCENARIO

In the highly correlated scenario, the power allocation problem can be formulated as

$$\max_{P_{u,m}} \frac{\alpha_L W}{N_c} \sum_{m=1}^{N_c} \log_2(1 + \frac{P_{1,m}\sigma_{1,m}^2}{\sigma_{\mathrm{n}}^2})$$
$$s.t. \sum_{u\in\Omega_m} P_{u,m} = P, \quad m = 1, 2, \ldots, N_c. \tag{28}$$

It can be seen that only the first equivalent channel in each spatial symbol contributes to the channel capacity. Thus all the power is allocated to the first equivalent channel to maximize the channel capacity, which is given as

$$C_{\mathrm{H}} = \frac{\alpha_L W}{N_c} \sum_{m=1}^{N_c} \log_2(1+\frac{P\sigma_{1,m}^2}{\sigma_{\mathrm{n}}^2}) + \alpha_L W \log_2 \frac{N_t!}{N_a!(N_t-N_a)!}. \tag{29}$$

Similar to the rich scattering scenario, on condition that the channel capacity remains the same with different spatial-domain symbols, the expression can be further simplified with the Stirling's approximation. Thus the approximation of the channel capacity is given as

$$C_{\mathrm{H}} \approx \alpha_L W[\log_2(1 + \frac{P\sigma_1^2}{\sigma_{\mathrm{n}}^2}) + (N_t+\frac{1}{2})\log_2(N_t) - \frac{\log_2(2\pi)}{2}$$
$$- (N_t - N_a + \frac{1}{2})\log_2(N_t - N_a) - (N_a + \frac{1}{2})\log_2(N_a)]. \tag{30}$$

Thus the optimal N_a can be derived by maximizing (30) through many numerical iterative methods.

B. LACO-OFDM BASED TIME-DOMAIN DIMMING

Similar to [19], the illumination level of the VLC system can be defined as

$$\eta = \frac{\sum_{i=1}^{N_a} \mathbb{E}[I_i]}{(I_{\mathrm{H}} - I_{\mathrm{L}})N_t} \times 100\%, \tag{31}$$

where $\mathbb{E}[\cdot]$ and I_i denote the expectation operator and the current for the i-th LED. Thus if a specific illumination requirement η is given, the sum of the expectations of the currents is limited as

$$\sum_{i=1}^{N_a} \mathbb{E}[I_i] = \eta(I_{\mathrm{H}} - I_{\mathrm{L}})N_t. \tag{32}$$

Due to the central limit theorem, the positive and negative LACO-OFDM symbols in the l-th layer follow the clipped Gaussian distribution [26]. The expectation of the ACO-OFDM signal is $\sigma_i^{(l)}/\sqrt{2\pi}$ in the i-th LED and the l-th layer, where $\sigma_i^{(l)}$ denotes the root mean square of the unclipped symbols in the i-th LED and the l-th layer. Thus after the bias adding as in (9) and (10), the expectations of the two kinds of symbols are given as

$$\begin{aligned}\mathbb{E}[I_i^{\mathrm{PLACO}}] &= I_{\mathrm{L}} + \mathbb{E}[s_{i,n}^{\mathrm{PLACO}}] \\ &= I_{\mathrm{L}} + \mathbb{E}[\sum_{l=1}^{L} s_{i,n}^{(l)}] \\ &= I_{\mathrm{L}} + \sum_{l=1}^{L} \sigma_i^{(l)}/\sqrt{2\pi} \\ &= I_{\mathrm{L}} + \tilde{I}_i,\end{aligned} \tag{33}$$

and similarly,

$$\mathbb{E}[I_i^{\mathrm{NLACO}}] = I_{\mathrm{H}} - \sum_{l=1}^{L} \sigma_i^{(l)}/\sqrt{2\pi} = I_{\mathrm{H}} - \tilde{I}_i, \tag{34}$$

where I_i^{PLACO} and I_i^{NLACO} denote the currents of the positive and negative LACO-OFDM symbols in the i-th LED, respectively. $\sum_{l=1}^{L} \sigma_i^{(l)}/\sqrt{2\pi}$ is denoted as $\tilde{I}_i$ for convenience. $\sigma_i^{(l)}$ in the i-th LED and l-th layer is given by the optimal power allocation.

If we denote the proportion of the positive LACO-OFDM symbols in a frame as $\alpha(0 \le \alpha \le 1)$ for all the LEDs. Thus the expectation of I_i is given as

$$\mathbb{E}[I_i] = \alpha(I_{\mathrm{L}} + \tilde{I}_i) + (1 - \alpha)(I_{\mathrm{H}} - \tilde{I}_i). \tag{35}$$

We substitute (35) into (32), and the proportion α is given as

$$\alpha = \begin{cases} 1, & \eta < \eta_{\min} \\ \dfrac{\eta(I_{\mathrm{H}}-I_{\mathrm{L}})N_t - N_a I_{\mathrm{H}} + \sum_{i=1}^{N_a} \tilde{I}_i}{N_a(I_{\mathrm{L}}-I_{\mathrm{H}}) + \sum_{i=1}^{N_a} 2\tilde{I}_i}, & \eta_{\min} \le \eta \le \eta_{\max} \\ 0, & \eta > \eta_{\max}. \end{cases} \tag{36}$$

The thresholds $\eta_{\min}$ and $\eta_{\max}$ are further given as

$$\eta_{\min} = \frac{N_a I_{\mathrm{H}} - \sum_{i=1}^{N_a} \tilde{I}_i}{(I_{\mathrm{H}} - I_{\mathrm{L}})N_t}, \tag{37}$$

and

$$\eta_{\max} = \frac{N_a I_{\mathrm{L}} + \sum_{i=1}^{N_a} \tilde{I}_i}{(I_{\mathrm{H}} - I_{\mathrm{L}})N_t}. \tag{38}$$

It can be seen that for low dimming requirement $\eta < \eta_{\min}$, α is set to 1, which means only positive LACO-OFDM symbols are used. While for high dimming requirement $\eta > \eta_{\max}$, only negative LACO-OFDM symbols are utilized. For intermediate illumination requirement, both positive and negative symbols are transmitted with proportion α. Thus the illumination level of the system η is controlled according to the illumination requirements.

V. SIMULATION RESULTS

In this section, several simulations are provided to substantiate the superior performance of the proposed scheme. The GenSM based VLC system using positive and negative LACO-OFDM symbols with dimming control is considered. The simulation parameters are summarized in Table 1. Since the channel capacity is related with the singular value of

TABLE 1. Simulation parameters.

Parameter	Explication	Value[a]
I_L	Minimum current level	0 A
I_H	Maximum current level	1 A
W	Bandwidth of LEDs	4 MHz
N	Number of subcarriers	64
L	Number of LACO-OFDM layers	3
P	Total transmit power	1 W
n_r	Refractive index	1.5
$\Phi_{1/2}$	Semiangle of transmitter	60°
Ψ_c	Semiangle of receiver FOV	90°
A	Area of PDs	1 cm^2

[a] A = ampere, Hz = hertz, W = watt, cm = centimeter.

channel matrix $\mathbf{H}$, in the rich scattering scenario, where the channels of the LEDs and PDs are supposed to be independent with each other, a Rayleigh fading channel, where each element $h_{i,j}$ in the channel matrix $\mathbf{H}$ follows an independent and identical standard Gaussian distribution $h_{i,j} \sim \mathcal{N}(0, 1)$, is adopted in the simulation to show the performance. While in the highly correlated scenario, the channels of LEDs and PDs are highly correlated with each other and the rank of the channel matrix degenerates to 1. Thus each line of $\mathbf{H}$ can be seen as a linear combination of the first row $\mathbf{h}_1$ of $\mathbf{H}$. In $\mathbf{h}_1$, each element also follows an independent and identical standard Gaussian distribution, which is $\mathbf{h}_1 \sim \mathcal{N}(\mathbf{0}, \mathbf{I}_{N_t})$.

The channel capacity of the proposed scheme in the rich scattering scenario is investigated in Fig. 2. The transmitter and receiver are equipped with $N_t = 16$ LEDs and $N_r = 16$ PDs, respectively. N_a LEDs are activated to transmit signals at the same time, and thus the number of different spatial-domain symbols is $N_c = \binom{16}{N_a}$. It is intuitive that the channel capacity raises with the increase of the SNR of the whole system, which is defined as $\gamma = P/\sigma_n^2$. The approximated optimal N_a derived by the proposed approximation of the channel capacity in (27) is also illuminated in Fig. 2. It can be seen that the approximation of the optimal N_a is accordant with the real value. Thus the proposed approximation can be utilized to derive the optimal N_a with high accuracy.

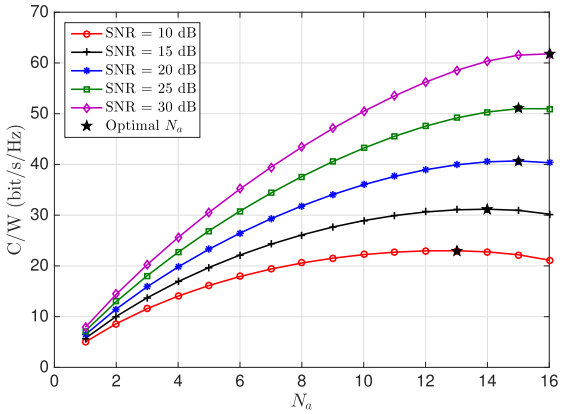


FIGURE 2. Comparison of the channel capacity versus the number of activated LEDs in the rich scattering scenario, where $N_t = N_r = 16$.

The channel capacity in the rich scattering scenario is further investigated with less LEDs and PDs in Fig. 3.

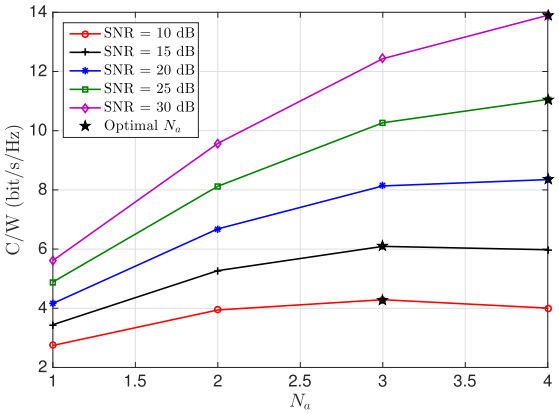


FIGURE 3. Comparison of the channel capacity versus the number of activated LEDs in the rich scattering scenario, where $N_t = N_r = 4$.

The transmitter and receiver are equipped with $N_t = 4$ LEDs and $N_r = 4$ PDs, respectively. It can be seen that the channel capacity in Fig. 3 is much lower than that in Fig. 2 under the same SNR and N_a, which is because the mutual information carried by the spatial-domain symbols is much lower with less optional LEDs. It can also be seen from the two figures that the optimal N_a raises with the increase of SNR. That is because the mutual information carried by the QAM symbols is larger than the mutual information carried by the spatial-domain symbols in high SNR region, thus more LEDs are activated to realize higher channel capacity.

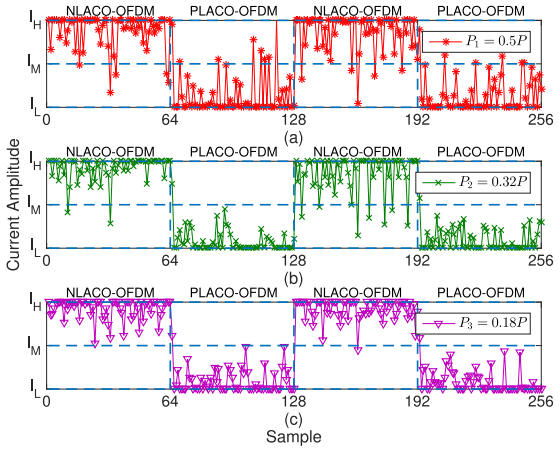


FIGURE 4. Illustration of the transmitted positive and negative LACO-OFDM symbols, where $\alpha = 0.5$.

An illumination of the transmitted positive and negative LACO-OFDM symbols is given in Fig. 4, where the SNR is 15 dB. In the first step of the proposed hybrid dimming scheme, the optimal number of activated LED is derived as $N_a = 3$ and the corresponding power allocation is obtained as $P_1 = 0.5P, P_2 = 0.32P, P_3 = 0.18P$ based on the maximization of the channel capacity. In the second step, the proportion of the positive LACO-OFDM symbols is derived as $\alpha = 0.5$ according to the given illumination requirements. It can be seen that half of the symbols are

positive LACO-OFDM symbols and the expectation of the current amplitude in the three LEDs are different based on the optimal power allocation.

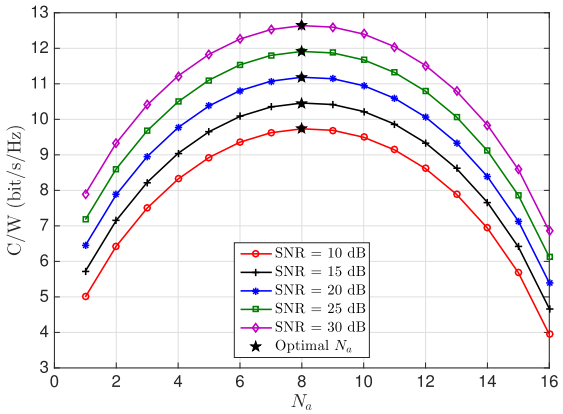


FIGURE 5. Comparison of the channel capacity versus the number of activated LEDs in the highly correlated scenario, where $N_t = N_r = 16$.

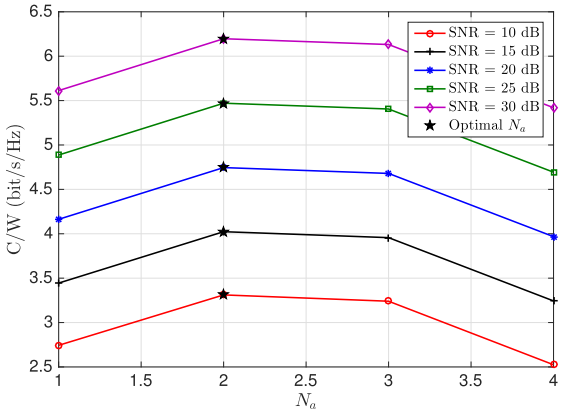


FIGURE 6. Comparison of the channel capacity versus the number of activated LEDs in the highly correlated scenario, where $N_t = N_r = 4$.

In Fig. 5 and Fig. 6, the channel capacities in the highly correlated scenario with different numbers of activated LEDs are investigated. The numbers of LEDs and PDs are $N_t = N_r = 16$ and $N_t = N_r = 4$, respectively. Compared to Fig. 2 and Fig. 3, it can be seen that the channel capacity in the highly correlated scenario is much smaller than the rich scattering scenario because the multiplexing gain of the multi-LED declines a lot with high channel correlation as shown in (30). The simulation results also demonstrate that the spatial-domain information dominates the trend of the capacity, which is because with high channel correlation, the multiplexing gain cannot raise with the increase of the number of activated LEDs. It is worth noting that the optimal N_a is derived accurately in the proposed scheme to maximum the channel capacity under different SNRs, LEDs, and PDs.

In Fig. 7, the channel capacities under different illumination levels in the rich scattering scenario and the highly correlated scenario are evaluated, respectively. The DCO-OFDM based hybrid dimming scheme with repetition coding (RC)

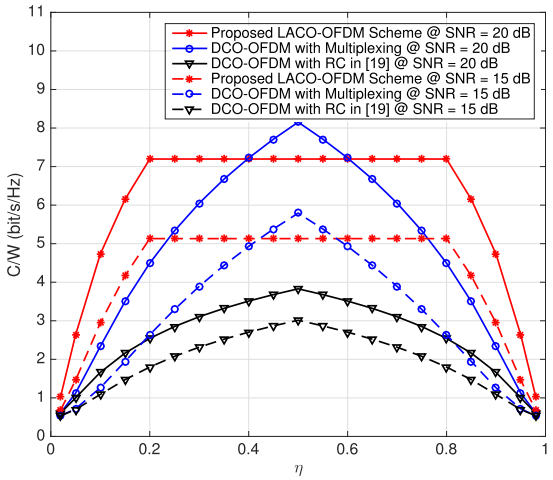


FIGURE 7. Comparison of the channel capacity versus the illumination levels in the rich scattering scenario, where $N_t = N_r = 4$.

in [19] and DCO-OFDM based hybrid dimming with spatial multiplexing are also investigated as comparison. The SNRs are set to be 20 dB and 15 dB. The optimal N_a is derived as 3 based on the maximization of the channel capacity as shown in Fig. 3. It can be seen that in the rich scattering scenario, the proposed hybrid dimming scheme outperforms the DCO-OFDM based scheme with RC in [19], which is because of the optimal power allocation and the optimal N_a selection in the proposed scheme. In the illumination requirement around $\eta = 0.5$, the DCO-OFDM based scheme with multiplexing shows higher channel capacity than the other schemes since it utilizes more subcarriers and exploits the whole dynamic range. However, the proposed scheme achieves superior channel capacity with lower and higher dimming requirements, because the whole dynamic range of the LEDs is utilized by both the conventional PLACO-OFDM and the novel NLACO-OFDM.

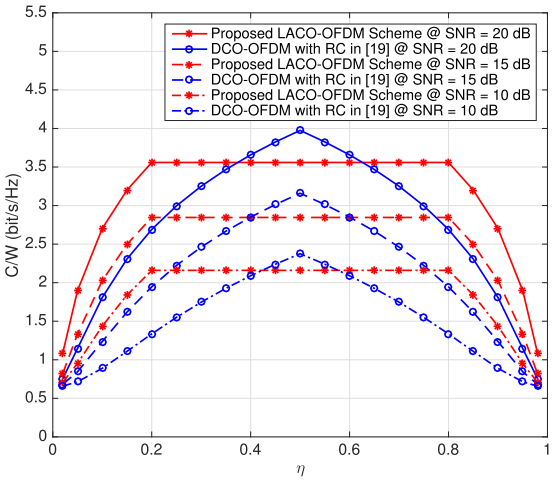


FIGURE 8. Comparison of the channel capacity versus the illumination levels in the highly correlated scenario, where $N_t = N_r = 4$.

The channel capacity under different illumination levels in the highly correlated scenario is investigated in Fig. 8.

The SNRs are set to be 20 dB, 15 dB, and 10 dB. The optimal N_a is derived as 2 according to Fig. 6. It can be seen that the channel capacity decreases a lot due to the decline in the multiplexing gain in the highly correlated scenario. The proposed GenSM based scheme with LACO-OFDM can provide higher channel capacity under much wider illumination requirements. Besides, the DC bias and scaling factor of the proposed hybrid dimming scheme need no adjustment under different dimming requirements at the receiver, which reduces the complexity of the demodulation process. In summary, the proposed GenSM based hybrid dimming scheme can provide high speed data transmission under much more diversified dimming requirements, which can achieve better balance between the illumination and the communication.

VI. CONCLUSION

The novel spectral-efficient GenSM based hybrid dimming scheme with LACO-OFDM was proposed in this paper for VLC. The channel capacities of the proposed scheme were analyzed and closed-form expressions of the channel capacity were derived in both the rich scattering scenario and the highly correlated scenario. Based on the maximization of the channel capacity, the two-step hybrid dimming scheme in both spatial and time domains was further proposed to realize flexible dimming control and high spectral efficient communication. In the end, the superior performance of the proposed dimming scheme over the state-of-art spatial dimming schemes was verified via numerical simulations.

REFERENCES

[1] A. Jovicic, J. Li, and T. Richardson, "Visible light communication: Opportunities, challenges and the path to market," *IEEE Commun. Mag.*, vol. 51, no. 12, pp. 26–32, Dec. 2013.

[2] L. Grobe *et al.*, "High-speed visible light communication systems," *IEEE Commun. Mag.*, vol. 51, no. 11, pp. 60–66, Dec. 2013.

[3] M. Z. Chowdhury, M. T. Hossan, A. Islam, and Y. M. Jang, "A comparative survey of optical wireless technologies: Architectures and applications," *IEEE Access*, vol. 6, pp. 9819–9840, 2018.

[4] D. Karunatilaka, F. Zafar, V. Kalavally, and R. Parthiban, "LED based indoor visible light communications: State of the art," *IEEE Commun. Surveys Tuts.*, vol. 17, no. 3, pp. 1649–1678, 3rd Quart., 2015.

[5] P. H. Pathak, X. Feng, P. Hu, and P. Mohapatra, "Visible light communication, networking, and sensing: A survey, potential and challenges," *IEEE Commun. Surveys Tuts.*, vol. 17, no. 4, pp. 2047–2077, 4th Quart., 2015.

[6] K. Cai, M. Jiang, and X. Ma, "Photodetector selection aided multiuser MIMO optical OFDM imaging visible light communication system," *IEEE Access*, vol. 4, pp. 9870–9879, 2016.

[7] W. O. Popoola, E. Poves, and H. Haas, "Error performance of generalised space shift keying for indoor visible light communications," *IEEE Trans. Commun.*, vol. 61, no. 5, pp. 1968–1976, May 2013.

[8] M. Di Renzo, H. Haas, A. Ghrayeb, S. Sugiura, and L. Hanzo, "Spatial modulation for generalized MIMO: Challenges, opportunities, and implementation," *Proc. IEEE*, vol. 102, no. 1, pp. 56–103, Jan. 2014.

[9] E. Curry and D. K. Borah, "Iterative combinatorial symbol design for spatial modulations in MIMO VLC systems," *IEEE Photon. Technol. Lett.*, vol. 30, no. 5, pp. 483–486, Mar. 1, 2018.

[10] B. Zhuang, C. Li, and Z. Xu, "Enhanced performance of spatial modulation with angular diversity receiver for indoor visible light communication," in *Proc. IEEE/CIC Int. Conf. Commun. China (ICCC)*, Jul. 2016, pp. 1–6.

[11] C. R. Kumar and R. K. Jeyachitra, "Dual-mode generalized spatial modulation MIMO for visible light communications," *IEEE Commun. Lett.*, vol. 22, no. 2, pp. 280–283, Feb. 2018.

[12] F. Wang *et al.*, "Secrecy analysis of generalized space-shift keying aided visible light communication," *IEEE Access*, vol. 6, pp. 18310–18324, 2018.

[13] S. Yao, X. Zhang, H. Qian, and X. Luo, "Joint dimming and data transmission optimization for multi-user visible light communication system," *IEEE Access*, vol. 5, pp. 5455–5462, 2017.

[14] F. Zafar, D. Karunatilake, and R. Parthiban, "Dimming schemes for visible light communication: The state of research," *IEEE Wireless Commun.*, vol. 22, no. 2, pp. 29–35, Apr. 2015.

[15] K. Lee and H. Park, "Modulations for visible light communications with dimming control," *IEEE Photon. Technol. Lett.*, vol. 23, no. 16, pp. 1136–1138, Aug. 15, 2011.

[16] J. Kim and H. Park, "A coding scheme for visible light communication with wide dimming range," *IEEE Photon. Technol. Lett.*, vol. 26, no. 5, pp. 465–468, Mar. 1, 2014.

[17] E. Cho *et al.*, "NRZ-OOK signaling with LED dimming for visible light communication link," in *Proc. 16th Eur. Conf. Netw. Opt. Commun.*, Jul. 2011, pp. 32–35.

[18] Y. Yang, Z. Zeng, J. Cheng, and C. Guo, "Spatial dimming scheme for optical OFDM based visible light communication," *Opt. Express*, vol. 24, no. 26, pp. 30254–30263, Dec. 2016.

[19] Y. Yang, Z. Zeng, J. Cheng, and C. Guo, "A novel hybrid dimming control scheme for visible light communications," *IEEE Photon. J.*, vol. 9, no. 6, Dec. 2017, Art. no. 7908312.

[20] A. H. Azhar, T.-A. Tran, and D. O'Brien, "A gigabit/s indoor wireless transmission using MIMO-OFDM visible-light communications," *IEEE Photon. Technol. Lett.*, vol. 25, no. 2, pp. 171–174, Jan. 15, 2013.

[21] J. B. Carruthers and J. M. Kahn, "Multiple-subcarrier modulation for nondirected wireless infrared communication," *IEEE J. Sel. Areas Commun.*, vol. 14, no. 3, pp. 538–546, Apr. 1996.

[22] J. Armstrong and A. J. Lowery, "Power efficient optical OFDM," *Electron. Lett.*, vol. 42, no. 6, pp. 370–372, Mar. 2006.

[23] B. Ranjha and M. Kavehrad, "Hybrid asymmetrically clipped OFDM-based IM/DD optical wireless system," *IEEE/OSA J. Opt. Commun. Netw.*, vol. 6, no. 4, pp. 387–396, Apr. 2014.

[24] Q. Wang, C. Qian, X. Guo, Z. Wang, D. G. Cunningham, and I. H. White, "Layered ACO-OFDM for intensity-modulated direct-detection optical wireless transmission," *Opt. Express*, vol. 23, no. 9, pp. 12382–12393, May 2015.

[25] F. Yang, Y. Sun, and J. Gao, "Adaptive LACO-OFDM with variable layer for visible light communication," *IEEE Photon. J.*, vol. 9, no. 6, Dec. 2017, Art. no. 7907908.

[26] F. Yang and J. Gao, "Dimming control scheme with high power and spectrum efficiency for visible light communications," *IEEE Photon. J.*, vol. 9, no. 1, Feb. 2017, Art. no. 7901612.

[27] L. Zeng, D. O'Brien, H. Le-Minh, K. Lee, D. Jung, and Y. Oh, "Improvement of date rate by using equalization in an indoor visible light communication system," in *Proc. 4th IEEE Int. Conf. Circuits Syst. Commun. (ICCSC)*, Shanghai, China, May 2008, pp. 678–682.

[28] L. He, J. Wang, and J. Song, "On generalized spatial modulation aided millimeter wave MIMO: Spectral efficiency analysis and hybrid precoder design," *IEEE Trans. Wireless Commun.*, vol. 16, no. 11, pp. 7658–7671, Nov. 2017.

[29] W. Zeng, C. Xiao, M. Wang, and J. Lu, "Linear precoding for finite-alphabet inputs over MIMO fading channels with statistical CSI," *IEEE Trans. Signal Process.*, vol. 60, no. 6, pp. 3134–3148, Jun. 2012.



TENGJIAO WANG was born in Henan, China, in 1993. He received the B.S. degree from the Department of Electronic Engineering, Tsinghua University, Beijing, China, in 2016. He is currently pursuing the Ph.D. degree with the DTV Technology R&D Center, Department of Electronic Engineering, Tsinghua University. His research interests lie in the field of visible light communications, 5G wireless technologies, multiple-input multiple-output systems, non-orthogonal multiple access, and sparse signal processing theory in wireless communications.



FANG YANG (M'11–SM'13) received the B.S.E. and Ph.D. degrees in electronic engineering from Tsinghua University, Beijing, China, in 2005 and 2009, respectively. He is currently an Associate Professor with the Research Institute of Information Technology, Tsinghua University. He has authored over 120 peer-reviewed journal and conference papers. He holds over 40 Chinese patents and two PCT patents. His research interests lie in the fields of channel coding, channel estimation, interference cancellation, and signal processing techniques for communication system, especially in power line communication, visible light communication, and digital television terrestrial broadcasting. He received the IEEE Scott Helt Memorial Award (Best Paper Award in the IEEE TRANSACTIONS IN BROADCASTING) in 2015. He is the Secretary General of Sub-Committee 25 of the China National Information Technology Standardization (SAC/TC28/SC25).



LING CHENG (M'10–SM'15) received the degree B.Eng. degree *(cum laude)* in electronics and information from the Huazhong University of Science and Technology (HUST) in 1995, and the M.Ing. *(cum laude)* and D.Ing. degrees in electrical and electronics from the University of Johannesburg in 2005 and 2011, respectively. His research interests are in digital communications and information theory. In 2010, he joined the University of the Witwatersrand, where he was promoted to an Associate Professor in 2015. He has been a visiting professor at four universities and the principal advisor for over 30 full research post-graduate students. He has authored over 60 research papers in journals and conference proceedings. He was a recipient of the Chancellor's Medal in 2005 and the National Research Foundation Rating in 2014. The IEEE ISPLC 2015 Best Student Paper Award was presented to his Ph.D. student in Austin, TX, USA. He has been serving as the Secretary for the IEEE South African Information Theory Chapter since 2012.



JIAN SONG (M'06–SM'10–F'16) received the B.Eng. and Ph.D. degrees in electrical engineering from Tsinghua University, Beijing, China, in 1990 and 1995, respectively. He was with Tsinghua University upon his graduation. He was with The Chinese University of Hong Kong and the University of Waterloo, Canada, in 1996 and 1997, respectively. He has been with Hughes Network Systems, USA, for seven years. He joined the Faculty Team, Tsinghua, as a Professor in 2005. He is currently the Director of the DTV Technology Research and Development Center, Tsinghua University. He has been working in quite different areas of fiber-optic, satellite, and wireless communications, and the power line communications. He has authored over 200 peer-reviewed journal and conference papers. He holds two U.S. and over 40 Chinese patents. His current research interest is in the area of digital TV broadcasting. He is fellow of the IET.